applied sciences

MDPI

Perspective

A Review of Mixture Theory for Deformable Porous Media and Applications

Javed Iqbal Siddique [1], Aftab Ahmed [2], Asim Aziz [3] and Chaudry Masood Khalique [4,*]

1 Department of Mathematics, York Campus, Penn State University, York, PA 17403-3326, USA; jis15@psu.edu
2 Department of Mathematics, Capital University of Science and Technology, Islamabad 44000, Pakistan; 680aftab@gmail.com
3 College of Electrical and Mechanical Engineering, National University of Sciences and Technology, Islamabad 44000, Pakistan; aaziz@ceme.nust.edu.pk
4 International Institute for Symmetry Analysis and Mathematical Modelling, Department of Mathematical Sciences, Mafikeng Campus, North-West University, Private Bag X 2046, Mmabatho 2735, South Africa
* Correspondence: Masood.Khalique@nwu.ac.za; Tel.: +27-18-389-2009

Received: 30 July 2017; Accepted: 4 September 2017; Published: 9 September 2017

Abstract: Mixture theory provides a continuum framework to model a multi-phase system. The basic assumption is, at any instant of time all phases are present at every material point and momentum and mass balance equations are postulated. This paper reviews the recent developments in mixture theory and focuses on the applications of the theory in particular areas of biomechanics, composite manufacturing and infiltration into deformable porous materials. The complexity based upon different permeability and stress functions is also addressed. The review covers the literature presented in the past fifty years and summarizes applications of mixture theory in specific areas of interest, for the sake of brevity, only necessary details are provided rather than complete modeling and simulation.

Keywords: mixture theory; deformable porous materials; compression moulding; biomechanics; capillary rise

1. Introduction

The deformation of the porous material due to fluid flow brings changes in physical properties such as permeability and porosity of the material. This ultimately alters the fluid flow through the porous material and develops a complex coupling between the matrix of porous material and fluid flow. This type of phenomena occurs in many industrial as well as biological settings and mathematical modeling of these processes is performed using the mixture theory. In mixture theory, individual components of the mixture, that is, solid matrix and a fluid can be modeled as superimposing continua so that each point in the solid-liquid mixture is occupied simultaneously by a material point of each constituent (see for example, Bedford and Drumheller [1]). The principals of modern mixture theory by using the continuum mechanics and proposing balance equations appropriate to mixtures irrespective of their constitution are formulated by Truesdell and Toupin [2], Truesdell [3,4] and Truesdell and Noll [5]. The detailed review of historical development of continuum theories of mixture is presented by Atkin and Craine [6] in 1976. The main focus of the present paper to present a review of the work done after 1976, while special emphases is given on the applications of mixture theory in deformable materials.

The first study of fluid flow through deformable porous material was presented by Terzaghi et al. [7]. Later on, Biot [8] studied the problem of soil consolidation where Darcy's law was used to describe the fluid flow coupled with linear elasticity model for solid deformation. This paved the path for further work of Biot [9,10], used extensively in soil mechanics. Biot's theory for deformable

porous media was then combined with the mixture theory to investigate the compressive behavior of articular cartilage by Mow, Lai and other co-authors [11–13] in 1980s. The general framework of the mixture theory is presented in the next section. In Section 3, application and literature survey of the theory in fluid flow through porous biological tissues, compression moulding process in connection with composite manufacturing process and capillary rise phenomena are presented. The detailed literature survey on applications of mixture theory in allied areas of sciences and engineering are given in Section 4. Finally, concluding remarks are furnished in Section 5.

2. Mixture Theory: General Framework

The continuum theory of mixtures is based on the notion that each constituent of the mixture is continuous and occupies every point in the space at each instant of time. The mixture theory described here is based on the work of Bowen [14]. For completeness, we present some basic equations of mixture theory from where governing equations of different fields such as biomechanics, manufacturing processes, radial flows, can be derived.

The apparent densities of individual components of the mixture are defined as

$$\rho^{\eta} = \lim_{dV \to 0} \frac{dm^{\eta}}{dV} \tag{1}$$

where $\eta = s$ represents the solid phase and $\eta = \ell$ denotes the liquid phase. dm^{η} is the mass of the η phase in the small volume dV. The actual densities and relative porocities of each phase in the mixture are defined as

$$\rho_T^{\eta} = \lim_{dV^{\eta} \to 0} \frac{dm^{\eta}}{dV^{\eta}} \tag{2}$$

$$\phi^{\eta} = \lim_{dV \to 0} \frac{dV^{\eta}}{dV} \tag{3}$$

where dV^{η} is the small volume of the η phase. Using Equations (2) and (3) in Equation (1), the relation between density and porosity is given as

$$\rho^{\eta} = \phi^{\eta} \rho_T^{\eta} \tag{4}$$

Densities and porosities of the solid and fluid phase are related to each other by the relations

$$\rho^{s} + \rho^{\ell} = \rho \tag{5}$$

$$\phi^{s} + \phi^{\ell} = 1 \tag{6}$$

where ρ is the density of the mixture. In the absence of chemical reaction conservation of mass for solid and fluid phase derived from simple continuum mechanics are written as

$$\frac{\partial \rho^{s}}{\partial t} + \nabla \cdot (\rho^{s} \mathbf{v^{s}}) = 0 \tag{7}$$

$$\frac{\partial \rho^{\ell}}{\partial t} + \nabla \cdot (\rho^{\ell} \mathbf{v}^{\ell}) = 0 \tag{8}$$

Here $\mathbf{v^{s}}$ and $\mathbf{v}^{\ell}$ are velocities of the solid and fluid phase, respectively. Adding Equations (7) and (8) after using Equations (4) and (6), yields

$$\nabla \cdot \mathbf{v} = 0 \tag{9}$$

where

$$\mathbf{v} = \mathbf{v^s}\phi^s + \mathbf{v}^\ell\phi^\ell \tag{10}$$

is the macroscopic medium velocity.

The momentum balance for solid and fluid phase is given by

$$\rho^\eta\left(\frac{\partial \mathbf{v}^\eta}{\partial t} + (\mathbf{v}^\eta \cdot \nabla)\mathbf{v}^\eta\right) = \nabla \cdot \mathbf{T}^\eta + \rho^\eta \mathbf{b}^\eta + \boldsymbol{\pi^\eta} \tag{11}$$

In Equation (11) $\mathbf{T}^\eta$ is the stress tensor for the η phase, $\mathbf{b}^\eta$ the net body force and $\boldsymbol{\pi^\eta}$ the internal frictional interaction force between the solid and fluid phase. Neglecting the inertial term and body forces in Equation (11) gives

$$\nabla \cdot \mathbf{T}^\eta + \boldsymbol{\pi^\eta} = 0 \tag{12}$$

The stress tensors $\mathbf{T}^\eta$ and $\boldsymbol{\pi^\eta}$ can be defined as

$$\mathbf{T}^\eta = -\phi^\eta p\mathbf{I} + \boldsymbol{\sigma^\eta} \tag{13}$$

$$\boldsymbol{\pi^s} = -\boldsymbol{\pi}^\ell = K\left(\mathbf{v^s} - \mathbf{v}^\ell\right) - p\nabla\phi^s \tag{14}$$

where p is fluid pressure, $\mathbf{I}$ the identity tensor, $\boldsymbol{\sigma^\eta}$ the stress and K the drag coefficient of relative motion. Moreover, Newton's third law of internal frictional forces implies that $\boldsymbol{\pi^s} + \boldsymbol{\pi}^\ell = 0$. Using Equation (13) in Equation (12) and adding momentum equations of both phases, the following equation is given

$$\nabla \cdot \boldsymbol{\sigma} = \nabla p \tag{15}$$

The relation for $\boldsymbol{\pi^s}$ can be substituted into Equation (12) and using the relation from Equation (6), results into

$$\nabla \cdot \boldsymbol{\sigma} = K\left(\mathbf{v^s} - \mathbf{v}^\ell\right) + \phi^s\nabla p \tag{16}$$

$$0 = -K\left(\mathbf{v^s} - \mathbf{v}^\ell\right) + \phi^\ell\nabla p \tag{17}$$

The elimination of pressure term from these equations gives

$$\nabla \cdot \boldsymbol{\sigma} = \frac{1}{\kappa}\left(\frac{\partial \mathbf{u}}{\partial t} - \mathbf{v}\right) \tag{18}$$

where $\kappa = \frac{\rho_\ell^2}{K}$ is the permeability of the medium. Number of authors [11,15–21] have used different forms of permeability functions while analyzing the specifics of their research.

3. Applications of Mixture Theory

In this section, applications of mixture theory in specific areas of interest are presented. In particular, the fluid flow through porous biological tissues, compression moulding process in connection with composite manufacturing process and the capillary rise phenomena are analyzed. Only necessary details are provided rather than complete mathematical model and solution procedure. It is important to note that all the graphical results shown below are for non-dimensional systems and details are not shown here (Barry and Aldis [16], Siddique and Anderson [19] and Farina et al. [22]).

3.1. Flow Induced Deformation of Porous Biological Tissues

The modeling details of flow induced deformation from pressurized cavities in absorbing porous tissue (as presented by Barry and Aldis [16]) are reproduced in this section. The schematic diagram of the mathematical model under consideration is presented in Figure 1.

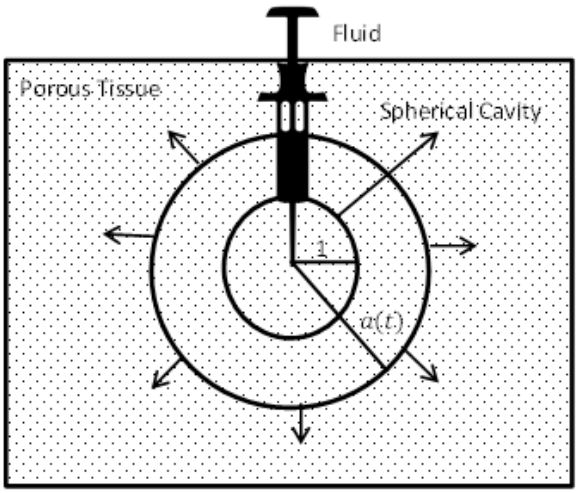

Figure 1. Radial flow after injection of fluid in an infinite porous media. The growth of cavity is occurring from radius 1 to $a(t)$.

The mathematical model is constructed under following assumptions:

- tissue to be deformable fully fluid saturated of infinite extent
- initially tissue is homogeneous and isotropic
- capillaries and lymphatics are distributed uniformly through the porous tissue
- tissue has ability to absorb the fluid at a rate proportional to local pressure.

Using above assumptions the Equations (7), (8), (15) and (18), the equation for fluid pressure p is written

$$\frac{\partial p}{\partial t} = \frac{\alpha}{r^2}\frac{\partial}{\partial r}\left\{ r^2 \kappa(p\delta)\frac{\partial p}{\partial r} \right\} - \beta p \tag{19}$$

where β is proportionality constant and contribution of this term in the continuity equation comes from the assumption of fluid absorption in the tissue. The permeability of the porous tissue considered here is $\kappa(p) = e^{mp}$, with m as a material constant. Initial and boundary conditions for fluid pressure $p(r,t)$ are given by

$$p(r,0) = f(r) = 0, \quad p(a,t) = \Delta P(t) = 1, \quad p(r,t) \to 0 \quad \text{as} \quad r \to \infty \tag{20}$$

Displacement of solid $u(r,t)$ in terms of fluid pressure as derived from the relations $\phi = \frac{1}{r^2}\frac{\partial}{\partial r}(r^2 u)$, $p(r,t) = H_a \phi(r,t)$ and boundary conditions for solid displacement are given by

$$u(r,t) = \frac{\gamma}{r^2}\left\{ \int_{a(t)}^{r} s^2 p(s,t) ds + \frac{a^3(t)\Delta P(t)}{2(1-\lambda)} \right\} \tag{21}$$

Here $\alpha, \delta, \gamma, \lambda$ are dimensionless parameters. Equations (19) and (21) together with boundary conditions Equation (20) are now solved numerically for the fluid pressure $p(r,t)$ and solid displacement $u(r,t)$. The details of the solution procedure are not presented here.

In Figure 2, fluid pressure is plotted as a function of radial distance r at specific times $t = 2, 4, 6$. Graphs are generated for the constant, $m = 0$, as well as for the nonlinear permeability, $m = 4$. Generally the permeability parameter m is in the range 0–10 for biological tissues and the steady-state of the fluid pressure is achieved at time $t = 6$, this is shown by the solid curve in Figure 2. It is important to note that for the nonlinear permeability case pressure decays slowly with radial distance as compared to the constant permeability case. In addition, steady state for fluid pressure is achieved earlier for constant permeability than nonlinear permeability. Moreover the fluid pressure p and the dilatation ϕ are related directly by the relation $p(r,t) = H_a\phi(r,t)$, therefore Figure 2 also explains porosity as a function of radial distance. In general the fluid volume fraction in the tissue increases due to deformation of the porous material which results in an overall expansion of the porous material.

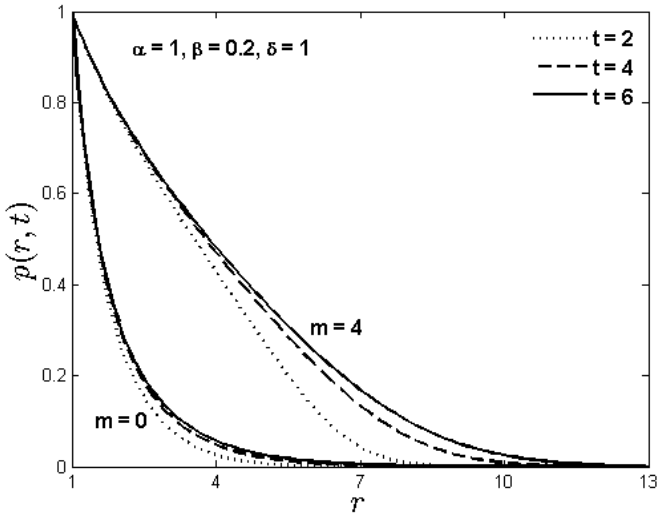

Figure 2. Fluid pressure as a function of radial distance for various values of time t and permeability parameter m.

Figure 3 presented the solid displacement $u(r,t)$ as a function of radial distance r at specific times $t = 2, 4, 6$. Numerical computations are carried for both constant, $m = 0$ and nonlinear permeability $m = 4$. It is noted that solid displacement falls exponentially with radial distance for constant permeability case whereas a definite inflection occurs in the displacement due to nonlinearities in permeability parameter m. Moreover, tissue solid displacement is increased for the nonlinear permeability as compared to the constant permeability. In addition in expanded pore region in Figure 3 is associated with the higher pressure and corresponding higher displacement. This is due to the coupled nature of solid permeability and displacement with fluid pressure decay.

In addition to the model presented here, Barry et al. [18,23–25] considered variety of different models involving deformable porous media based on mixture theory. These models include, for example, flow induced deformation of soft biological tissues, radial flow through deformable porous shells, unsteady flow induced deformation of porous materials and fluid flow over a thin deformable porous layer. In these models they developed one dimensional parabolic equations using spherical and cylindrical geometries and considered various permeability relations to account for the solid displacement. In general their main focus was to enhance the understanding of many complex biological phenomena occurring in soft tissue mechanics along with features that are usually missed due to absence of mixture theory modeling.

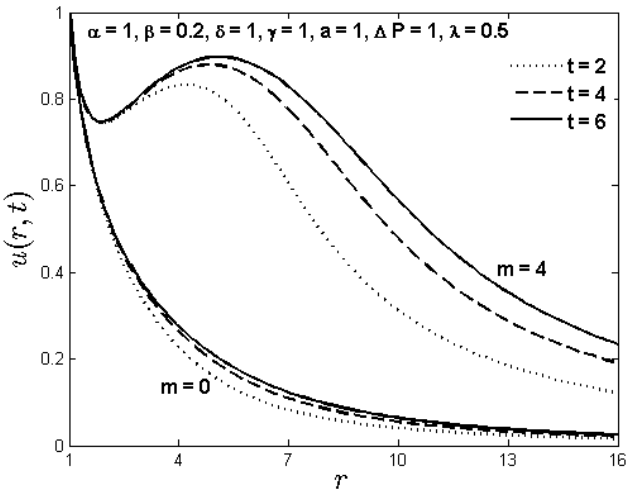

Figure 3. Solid displacement as a function of radial distance for various values of time t and permeability parameter m.

3.2. Mixture Theory Based Modelling and Simulation of Composite Manufacturing Processes

The application of mixture theory to model the manufacturing process of composite materials by compression moulding is discussed in this section. This is the process in which deformable porous material is pre–heated and then compressed. In particular, number of fibers are pre impregnated with certain quantity of liquid matrix possibly distributed in piles in a unidirectional or multidirectional way and finally placed among the porous mold. This generated mixture of solid and liquid is then heated and compressed by a piston which generates an increase in solid volume fraction and produces a flow in a deformable porous material. In this complex and fast process of compression moulding, the focus is to reduce the fabrication cost and should be accurate enough to reduce the chance of creating any inhomogeneities or damage to the solid. In general this process can be defined as a process of liquid flow through a deformable porous material and mixture theory equations for flow in deformable porous media can be helpful. The mathematical model and the associated examples are taken from the research article of Farina et al. [22]. The geometry of the flow model is given in Figure 4.

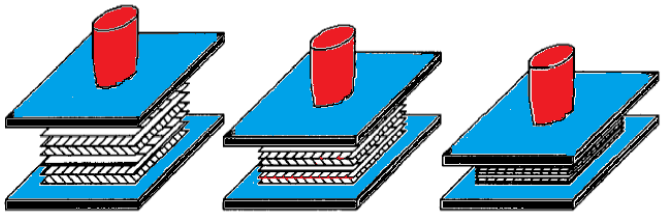

Figure 4. The schematic of a compression moulding process.

Here the set of mathematical equations are first written in Eulerian frame from Equations (7), (8) and (15) and then performed necessary mathematical manipulation steps to write down a partial differential equation in Eulerian frame on a time–varying domain along with moving boundary. These equations are difficult to handel numerically, therefore, Lagrangian coordinates are used to write down the following partial differential equation on a fixed solid matrix

$$\frac{\partial e}{\partial t} - \frac{(1+e^*)^2}{\mu}\frac{\partial}{\partial X}\left[\frac{K(e)}{(1+e)}\Sigma(e)\frac{\partial e}{\partial X}\right] = 0 \tag{22}$$

where $e = \frac{1-u}{u}$ and u is solid volume fraction. Here $K(e) = \alpha e^{\left(\frac{-\beta}{1+e}\right)}$, $\sigma(e) = \gamma[e^{\left(\frac{\delta}{1+e}\right)} - e^{\left(\frac{\delta}{1+e^*}\right)}]$ and $\Sigma(e) = \left|\frac{d\sigma(e)}{de}\right|$, where $\gamma = 0.3$ Pa, $\alpha = 1.5 \times 10^{-2}$ m^2, $\delta = 25$ and $\beta = 15$ are used in the simulation below.

Initial and boundary conditions for velocity and pressure driven dynamics are written as given by Farina et al. [22]

$$e(X,0) = e^*, \frac{\partial e(0,t)}{\partial X} = 0 \tag{23}$$

$$e(L^*,t) = \sigma^{-1}(P_0(t)) \quad \text{(for pressure driven dynamics)} \tag{24}$$

$$\frac{\partial e(L^*,t)}{\partial X} = -\frac{\mu}{K(e(L^*,t))\Sigma(e(L^*,t))}\frac{1+e(L^*,t)}{(1+e^*)}v_p(t) \quad \text{(for velocity driven dynamics)} \tag{25}$$

where μ is the liquid viscosity, L^* the initial height of wet prepreg, $P_0(t)$ the pressure applied on piston and $v_p(t)$ the piston velocity.

The above equations are then solved numerically after nondimensionalization and the results for solid volume fraction $u(Y,T)$ are shown in Figures 5 and 6. In particular, Figure 5 shows solid volume fraction u as a function of Lagrangian coordinate Y and normalized time T for velocity driven dynamics when $v_p(t) = 3[1 - \cos(20\pi T)]$. Note that $Y = 0$ indicates the piston surface whereas $Y = 1$ corresponds to the draining surface. The Figure 5 shows the compression of the porous material starts from the draining surface which we represent by $Y = 1$. When this part feels the load, the material under the piston shows compression after sometime. It is important to note that the solid volume fraction of the porous material attains homogeneous state after certain time.

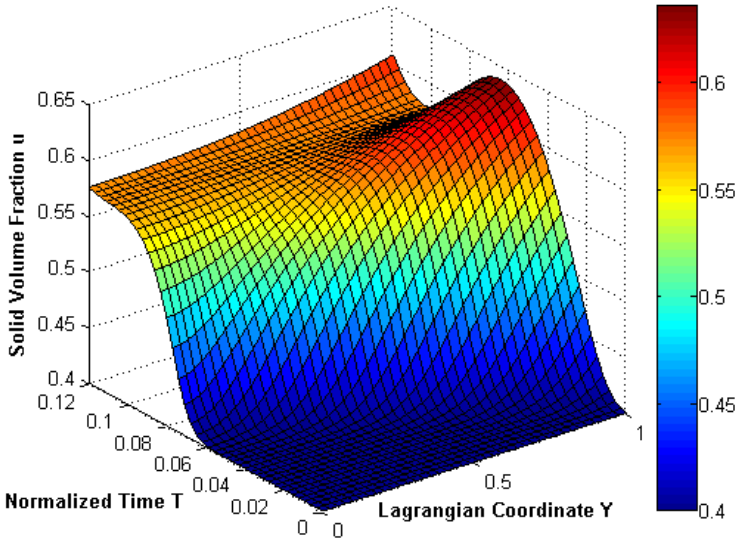

Figure 5. Solid volume fraction as a function of Lagrangian coordinate Y and normalized time T for piston velocity $v(T) = 3[1 - \cos(20\pi T)]$.

Figure 6 shows solid volume fraction u as a function of Lagrangian coordinate Y and normalized time T for pressure profile $P_0(t) = 1.25\sin(\frac{50\pi}{6}T)$. Again the process of compression starts from draining surface and the material surface goes through a steep increase of solid volume fraction. This quick growth in the pressure is related to the choice of the pressure function $P_0(t)$ which ultimately causes a rapid increase of solid fraction.

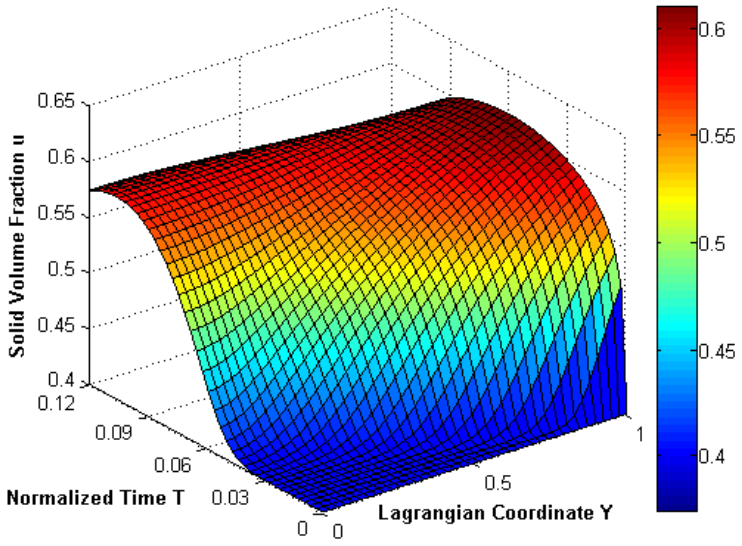

Figure 6. Solid volume fraction as a function of Lagrangian coordinate Y and normalized time T for pressure $p(T) = 1.25\sin(\frac{50\pi}{6}T)$.

Many composite manufacturing processes, such as resin transfer moulding, structural resin injection moulding and squeeze casting, can be considered as infiltration problems through an initially dry deformable porous material. Keeping in view some composite manufacturing processes, Preziosi et al. [26] investigated infiltration of an incompressible liquid in an initially dry, deformable porous media using mixture theory approach and good agreement between numerical simulation and experimental data was presented. This idea was then followed by many authors, for example, Ambrosi and Preziosi [15] and Billi and Farina [27]. It is important to mention that Preziosi [28] presented a great deal of review on composite manufacturing processes.

3.3. Unidirectional Capillary Rise into Deformable Porous Material

In this section a one-dimensional model of a sponge-like deformable porous material which is in contact with an infinite bath is discussed. The geometry of the model is shown in Figure 7. The porous material is initially dry and rigid having uniform solid volume fraction ϕ_0. The upper end of the deformable porous material is fixed and the contact position of porous material and liquid is represented by $z = 0$. The infiltration of liquid starts from infinite bath of liquid (i.e., $z = 0$) and the material's upper end is open to atmospheric pressure p_A. After time $t > 0$, the liquid starts to penetrate into initially dry porous material because of capillary forces associated with the pores of the porous material with the assumption that the capillary pressure $p_c < 0$, this causes the deformation in the porous material. The upper border of the wet porous material which we define as wet material–dry material interface $z = h_\ell(t)$ and the bottom border which develops after the imbibition of liquid which we define as liquid–wet material interface $z = h_s(t)$. The pressure of liquid bath is assumed to be hydrostatic, that is, $p = p_A - \rho_\ell g h_s$ at the solid liquid interface.

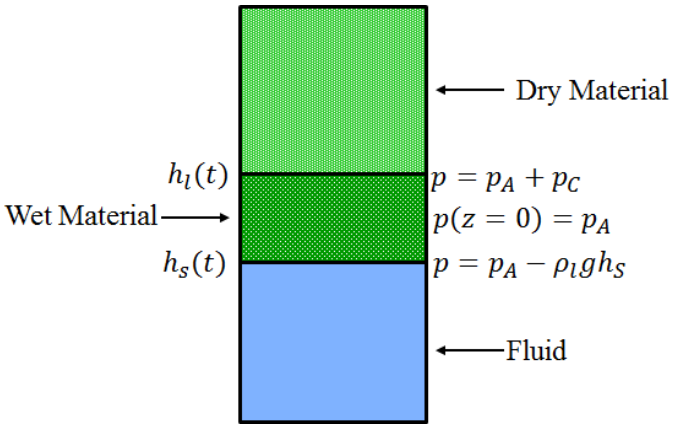

Figure 7. The dynamics of capillary rise after $t > 0$.

In the light of above assumptions, the set of Equations (7), (8), (15), and (17) for unidirectional capillary rise dynamics are obtained. The detailed equations are given in Siddique and Anderson [19]. It is important to note that for capillary rise dynamics Equation (15) in the presence of gravity effect takes the following form

$$\nabla p = \nabla \cdot \sigma + (\rho_s + \rho_\ell)\mathbf{g} \tag{26}$$

where ρ_s and ρ_ℓ are solid and liquid densities. After performing necessary mathematical manipulation steps Equations (7), (8), (17) along with (26) simplifies to the nonlinear partial differential equation (PDE) for solid volume fraction ϕ [19]

$$\frac{\partial \phi}{\partial t} + c(t)\frac{\partial \phi}{\partial z} = -\frac{\partial}{\partial z}\left[\phi k(\phi)\left\{\sigma'(\phi)\frac{\partial \phi}{\partial z} - \rho\phi\right\}\right] \tag{27}$$

The ordinary differential equations at the interface positions $h_s(t)$ and $h_\ell(t)$ are

$$\frac{dh_s}{dt} = c(t) + k(\phi)\left[\sigma'(\phi)\frac{\partial \phi}{\partial z} - \rho\phi\right]\Big|_{h_\ell^+} \tag{28}$$

$$\frac{dh_l}{dt} = c(t) - \frac{\phi k(\phi)}{(1-\phi)}\left[\sigma'(\phi)\frac{\partial \phi}{\partial z} - \rho\phi\right]\Big|_{h_\ell^-} \tag{29}$$

The function $c(t)$ that appears in Equations (27)–(29) has the following form [26]

$$c(t) = -\frac{(1-\phi_0)}{\phi_0}\left[\frac{\phi k(\phi)}{(1-\phi)}\left(\sigma'(\phi)\frac{\partial \phi}{\partial z} - \rho\phi\right)\right]\Big|_{h_\ell^-} \tag{30}$$

This completes the set of equations needed to capture the dynamics of capillary rise. Our attention here is to highlight two special cases with the help of above set of equations.

In the absence of gravity effects, the above systems of Equations (27)–(29) admits similarity solution and interested readers can find the related details in Siddique and Anderson [19] and Anderson [29]. When similarity variables is introduced in the above set of equations, the outcome is an ordinary differential equation (ODE) for solid volume fraction and algebraic equations for interface positions. Finally these ODEs along with the interface position yields error function solution for special choices of permeability function $k(\phi)$ and $\sigma(\phi)$ [29].

In the presence of gravity effects, the PDE (27) for solid volume fraction ϕ along with ODE Equations (28) and (29) is solved numerically. The details of numerical solution can be found in

both Siddique and Anderson [19] and Anderson [29] which is beyond the scope of this review article. The goal of this study is to present the resulting system of equations along with their numerical solution outcome for graphical representation. The graph for both zero and non-zero gravity solution is presented in Figure 8. In this plot the choice of permeability and solid stress are used as given in Siddique and Anderson [19]. It is evident from the Figure 8, for zero gravity case both solid $h_s(t)$ and liquid h_ℓ interface positions follow square root in time trend. In the presence of gravity effects, in the beginning both curves follow similarity solution and then deviate from this trend and reach to equilibrium solution. The limit of this presentation of these graphical results is up to this and readers are referred to Siddiqui et al. [20] for more details where steady state solution along with experimental comparison can be found.

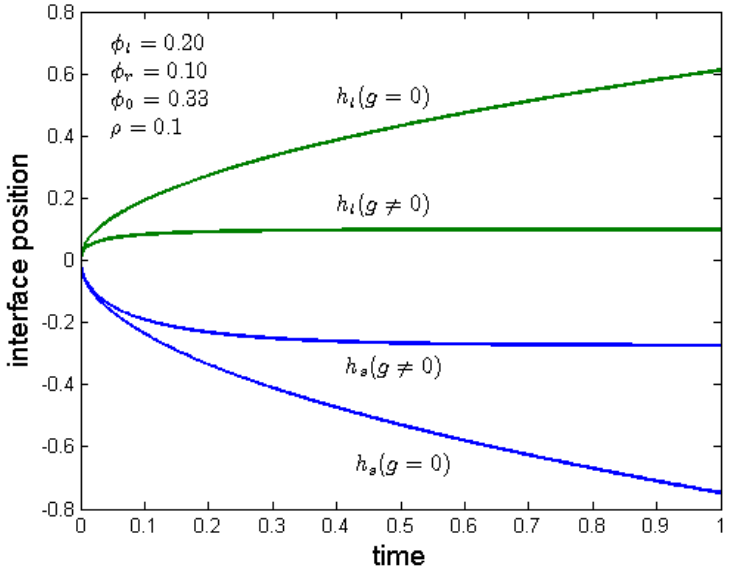

Figure 8. The dynamics of capillary rise for both zero and non–zero gravity cases.

Anderson [29] also studied the imbibition of a liquid droplet on a deformable porous substrate using mixture theory approach. In their model the gravity effects were not present and it is reported that imbibition of liquid into deformable porous material results into swelling, swelling relaxation, and shrinking. Later on, Siddique et al. [19,20,30] studied the capillary rise phenomena into a deformable sponge like material by including the gravity, power law and MHD fluid effects. On the similar lines, Sommer and Mortensen [31] studied unidirectional forced infiltration in an initially dry sponge like material. The fluid flow in this case was driven by a constant applied pressure and their predictions were compared with experimental results. A similar model of an infiltration for an initially dry and compressed porous material was presented by Preziosi et al. [26]. The section below contains literature review of mixture theory applications in other areas where we limit our self for summary rather then detailed modeling and simulation.

4. Further Applications of Mixture Theory

It is well known that organs, tissues and cells can be considered as mixture-composites, as they consist of multiple solid and fluid constituents. Therefore authors employed the idea of continuum mixture theory to describe the behaviors of soft biological tissues. Moreover, Growth and remodeling of porous biological tissues are studied by incorporating the effect of chemical reactions among mixture constituents. Humphrey [32] provided a comprehensive review of continuum biomechanics of soft biological tissues mentioning the work of Mow and Lai [11] and Mow et al. [12,13] for the development of biphasic mixture theory for biological tissues. The so-called linear biphasic theory considered cartilage as a solid which exhibited a linearly elastic isotropic response and the viscous

fluid. Extending the idea of biphasic to triphasic mixture theory, Lai et al. [33] developed mathematical models for soft tissues including the ion concentration as a third phase in addition to solid and fluid phase. Large numbers of papers [34–37] have been reported considering triphasic approach. Treating the ions in a mixture as a combination of cations and anions, a quardiphasic mixture theory for soft biological tissue was developed by Frijns et al. [38]. Holmes [39,40] has also contributed in mixture modeling of soft tissues particularly articular cartilage. Another important application of mixture theory in biomechanics is the resorption phenomena in bones reconstructed with bio-resorbable materials. Lekszycki and Isola et al. [41] presented a continuum poro-elastic mixture model where two apparent mass densities were introduced to describe the situations in which bone tissues and bio-resorbable materials coexist and interact. They focused on the final healing stage process until the bone is remodeled and eventually replaced by newly synthesised living tissue. A similar study was undertaken by Giorgio et al. [42] where a finite element analysis was carried out to investigate the phenomena of resorption and growth of bone tissue. The mixture theory approach is also followed by authors to include, for example, arterial tissue [21,43,44], cornea [45], skin [46] and lung [47].

Mathematical models based on mixture theory for the growth of tumors and the growth and remodeling of soft tissues were developed by many researchers, for example, Byrne and Preziosi [48], Ambrosi and Preziosi [49], Preziosi and Tosin [50] and Ambrosi et al. [51]. In the model of tumor growth, they considered avascular tumor as a mixture comprising of solid, cellular and liquid phase. Their novel feature includes the dependence of cell proliferation rate on the cellular stress and the incorporation of mass exchange between the two phases. In case of growth and remodeling of tissues, the emergence of residual stress is considered in the framework of mixture theory.

Cvetkovic et al. [52] studied the case of one-dimensional sedimentation using continuum mixture theory approach and developed the constitutive equations by using the method of Lagrangian multipliers. The governing diffusion equation for quasi-steady sedimentation is derived and analyzed to understand some physical aspect of the problem. Nayfeh [53] discussed the heat conduction in laminated composites using mixture theory. Governing equations for the actual composite are obtained and the cases of both harmonic and transient temperature pulses were considered in his work. Rosi et al. [54] considered an interesting application of the mixture theory by proposing a mathematical model involving a deformable porous media saturated by compressible nematic liquid crystal under slowly varying electric fields and assumed that the system follows a Biot-type model.

A two-phase mixture theory approach for the deflagration-to-detonation transition (DDT) in reactive granular materials was under taken by Baer and Nunziato [55] in 1986. They applied this model to describe combustion processes linked with DDT in a pressed column of HMX. Numerical simulations using method of lines were carried out to demonstrate the effect of particle size and porosity along with the study of bed compaction. Kirwan [56] presented a review of mixture theory with applications in physical oceanography and meteorology and discussed some examples which include turbidity currents, deforming sea beds, seawater and air containing all phases of water. By using the modern mixture theory, he also discussed the thermodynamics of a mixture of ice, water vapor and condensate in the atmosphere. Applications of continuum mixture theory to turbulent snow, air flows and sedimentation was also studied by Decker [57]. By making a constitutive assumption for the turbulent variables of the snow phase, governing non-linear partial differential equations were derived and then solved numerically using finite difference methods. In particular, snow phase velocity and density fields were investigated for different airflow regimes.

Del Bufalo et al. [58] used a mixture theory framework for modeling the mechanical actuation of ionic polymer metal composites (IPMC) in 2008. An IPMC is a porous charged polymer saturated with an electrolytic solvent and plated by two electrodes. Structural deformation was generated by applying voltage differences across the electrodes. Theoretical results were validated through a set of experiments performed on Nafion-based IPMCs. Applications of mixture theory in the fields such as consolidation problems, localization phenomena, drying processes, biomechanics, environmental mechanics, material science, local water supplies and analysis of plant growth were discussed in the

monograph by De Boer [59]. Chen [60] used the solid-fluid mixture theory to develop mathematical model describing the diffusion problems such as injection of fluid into a geological formation saturated with another fluid, drainage of two different fluids from a geological formation due to in-situ fluid pore pressure and the process of squeezing a sponge dry. A continuum theory for mixture of fluids and elastic solids interacting with electromagnetic (E-M) fields and superconductors was introduced by Eringen [61] in the year 1998. In particular, mechanical and E-M balance laws were postulated for mixture comprising of N-species. Species may be regular conductors or superconductors. Different combinations of mixture consisting of fluid-fluid, fluid-solid and solid-solid were considered and analyzed. A continuum model for shape memory alloys (SMA) was developed by Peng et al. [62] in 2001, which finds many practical applications in various fields.

Applications of mixture theory in the evaluation of mechanical properties of asphalt concrete were discussed by Wang et al. [63] and Krishnan and Rao [64,65]. Asphalt concrete used in flexible highway pavements include 5–8% air voids immediately after laying of the roadway. Rajagopal et al. [66] modeled electro-rheological material using mixture theory approach. Recent advances on theory of mixtures in geo-mechanics can be found in the book of Voyiadjis and Song [67].

5. Concluding Remarks

This review summarizes recent applications of mixture theory in different scientific fields. In particular, it is reported how mixture theory was applied to deformable porous materials to investigate the binary mixture comprising of solid and fluid phase. More specifically, flow-induced deformation of soft biological tissues, compression moulding process involving a deformable porous material and infiltration of liquid into sponge like material were discussed graphically from mixture theory viewpoint. The primary message, therefore, is merely that much has been done, but a great deal of work remains to be explored. Indeed, the constitutive relations, can be modeled in a better way to account for the description of most important behaviors of practical interest.

Acknowledgments: This material is based on the work supported by the Simons Foundation Grant No. 281839 and Penn State York.

Author Contributions: Javed Iqbal Siddique and Chaudhry Masood Khalique conceived and organize the research work; Aftab Ahmed and Asim Aziz performed the literature survey and write the paper.

Conflicts of Interest: The authors declare no conflict of interest.

References

1. Bedford, A.; Drumheller, D.S. Theories of immiscible and structured mixtures. *Int. J. Eng. Sci.* **1983**, *21*, 863–960.
2. Truesdell, C.; Toupin, R.A. The classical field theories of mechanics. In *Hand Book of Physics*; Springer: New York, NY, USA, 1960; Volume 3.
3. Truesdell, C. Sulle basi de la termomecanica. *Rend. Acad. Lincei* **1957**, *22*, 33–88. (In Italian)
4. Truesdell, C. *Rational Thermodynamics*, 2nd ed.; Springer: New York, NY, USA, 1984.
5. Truesdell, C.; Noll, W. The non-linear field theories of mechanics. In *The Non-Linear Field Theories of Mechanics*; Springer: New York, NY, USA, 2004; pp. 1–579.
6. Atkin, R.J.; Craine, R.E. Continuum theories of mixtures: Basic theory and historical development. *Q. J. Mech. Appl. Math.* **1976**, *29*, 209–244.
7. Terzaghi, K. *Erdbaumechanik auf Bodenphysikalischer Grundlage*; Franz Deuticke: Leipzig, Germany, 1925. (In German)
8. Biot, M.A. General theory of three dimensional consolidation. *J. Appl. Phys.* **1941**, *12*, 155–164.
9. Biot, M.A. Theory of elasticity and consolidation for a porous anisotropic solid. *J. Appl. Phys.* **1955**, *26*, 182–185.
10. Biot, M.A. Mechanics of deformation and acoustic propagation in porous media. *J. Appl. Phys.* **1962**, *33*, 1482–1498.
11. Mow, V.C.; Lai, W.M. Mechanics of animal joints. *Annu. Rev. Fluid Mech.* **1979**, *11*, 247–288.

12. Mow, V.C.; Kuei, S.C.; Lai, W.M.; Armstrong, C.G. Biphasic creep and stress relaxation of articular cartilage in compression: Theory and experiments. *J. Biomech. Eng.* **1980**, *102*, 73–84.
13. Mow, V.C.; Holmes, M.H.; Lai, W.M. Fluid transport and mechanical properties of articular cartilage: A review. *J. Biomech.* **1984**, *17*, 377–394.
14. Bowen, R.M. Incompressible porous media Models by use of the theory of mixtures. *Int. J. Eng. Sci.* **1980**, *18*, 1129–1148.
15. Ambrosi, D.; Preziosi, L. Modeling injection molding processes with deformable porous preforms. *SIAM J. Appl. Math.* **2000**, *61*, 22–42.
16. Barry, S.I.; Aldis, G.K. Flow-induced deformation from pressurized cavities in absorbing porous tissues. *Bull. Math. Biol.* **1992**, *54*, 977–997.
17. Anderson, D.M.; Siddique, J.I. Modeling wicking in deformable porous media using mixture theory. In *Wicking in Porous Materials: Traditional and Modern Modeling Approaches*; CRC Press: Boca Raton, FL, USA, 2012; p. 295.
18. Barry, S.I.; Aldis, G.K. Comparison of models for flow induced deformation of soft biological tissue. *J. Biomech.* **1990**, *23*, 647–654.
19. Siddique, J.I.; Anderson, D.M. Capillary rise of a non-Newtonian liquid into a deformable porous material. *J. Porous Media* **2011**, *14*, 1087–1102.
20. Siddique, J.I.; Anderson, D.M.; Bondarev, A. Capillary rise of a liquid into a deformable porous material. *Phys. Fluids* **2009**, *21*, 013106.
21. Klanchar, M.; Tarbell, J.M. Modeling water flow through arterial tissue. *Bull. Math. Biol.* **1987**, *49*, 651–669.
22. Farina, A.; Cocito, P.; Boretto, G. Flow in deformable porous media: modelling and simulations of compression moulding processes. *Math. Comput. Model.* **1997**, *26*, 1–15.
23. Barry, S.I.; Aldis, G.K. Radial flow through deformable porous shells. *J. Aust. Math. Soc. Ser. B* **1993**, *34*, 333–354.
24. Barry, S.I.; Aldis, G.K. Unsteady flow induced deformation of porous materials. *Int. J. Non-Linear Mech.* **1991**, *26*, 687–699.
25. Barry, S.I.; Parkerf, K.H.; Aldis, G.K. Fluid flow over a thin deformable porous layer. *Z. Angew. Math. Phys.* **1991**, *42*, 633–648.
26. Preziosi, L.; Joseph, D.D.; Beavers, G.S. Infiltration of initially dry, deformable porous media. *Int. J. Multiph. Flow* **1996**, *22*, 1205–1222.
27. Billi, L.; Farina, A. Unidirectional infiltration in deformable porous media: Mathematical modeling and self-similar solution. *Q. Appl. Math.* **2000**, *58*, 85–101.
28. Preziosi, L. The theory of deformable porous media and its application to composite materials manufacturing. *Surv. Math. Ind.* **1996**, *6*, 167–214.
29. Anderson, D.M. Imbibition of a liquid droplet on a deformable porous substrate. *Phys. Fluids* **2005**, *17*, 087104.
30. Siddique, J.I.; Kara, A. Capillary rise of magnetohydrodynamics liquid into deformable porous material. *J. Appl. Fluid Mech.* **2016**, *9*, 2837–2843.
31. Sommer, J.L.; Mortensen, A. Forced unidirectional infiltration of deformable porous media. *J. Fluid Mech.* **1996**, *311*, 193–217.
32. Humphrey, J.D. Continuum biomechanics of soft biological tissues. *Proc. R. Soc. Lond. A Math. Phys. Eng. Sci.* **2003**, *459*, 3–46.
33. Lai, W.M. Drag induced compression of articular cartilage during a permeation experiment. *J. Biorheol.* **1980**, *17*, 111–123.
34. Mow, V.C.; Kwan, M.K.; Lai, W.M.; Holmes, M.H. A finite deformation theory for nonlinearly permeable soft hydrated biological tissues. In *Frontiers in Biomechanics*; Springer: New York, NY, USA, 1986; pp. 153–179.
35. Lai, W.M.; Hou, J.S.; Mow, V.C. A triphasic theory for the swelling and deformation behaviors of articular cartilage. *J. Biomech. Eng.* **1991**, *113*, 245–258.
36. Ricken, T.; Schwarz, A.; Bluhm, J. A triphasic theory for growth in biological tissue-basics and applications. *Materialwiss. Werkstofftech.* **2006**, *37*, 446–456.
37. Myers, T.G.; Aldis, G.K.; Naili, S. Ion induced deformation of soft tissue. *Bull. Math. Biol.* **1995**, *57*, 77–98.
38. Frijns, A.J.H.; Huyghe, J.M.; Janssen, J.D. A validation of the quadriphasic mixture theory for intervertebral disc tissue. *Int. J. Eng. Sci.* **1997**, *35*, 1419–1429.

39. Holmes, M.H. A nonlinear diffusion equation arising in the study of soft tissue. *Q. Appl. Math.* **1983**, *41*, 209–220.
40. Holmes, M.H. Comparison theorems and similarity solution approximations for a nonlinear diffusion equation arising in the study of soft tissue. *SIAM J. Appl. Math.* **1984**, *44*, 545–556.
41. Lekszycki, T.; Dell'Isola, F. A mixture model with evolving mass densities for describing synthesis and resorption phenomena in bones reconstructed with bio-resorbable materials. *Z. Angew. Math. Mech.* **2012**, *92*, 426–444.
42. Giorgio, I.; Andreaus, U.; Scerrato, D.; Dell'Isola, F. A visco-poroelastic model of functional adaptation in bones reconstructed with bio-resorbable materials. *Biomech. Model. Mechanobiol.* **2016**, *15*, 1325–1343.
43. Kenyon, D.E. The theory of an incompressible solid-fluid mixture. *Arch. Ration. Mech. Anal.* **1976**, *62*, 131–147.
44. Jayaraman, G. Water transport in the arterial wall a theoretical study. *J. Biomech.* **1983**, *16*, 833–840.
45. Friedman, M.H. General theory of tissue swelling with application to the corneal stroma. *J. Theor. Biol.* **1971**, *30*, 93–109.
46. Oomens, C.W.J.; van Campen, D.H.; Grootenboer, H.J. A mixture approach to the mechanics of skin. *J. Biomech.* **1987**, *20*, 877–885.
47. Ford, T.R.; Sachs, J.S.; Grotberg, J.B.; Glucksberg, M.R. Mechanics of the perialveolar interstitium of the lung. In Proceedings of the First World Congress of Biomechanics, La Jolla, CA, USA, 30 August–4 September 1990; Volume 1, p. 31.
48. Byrne, H.; Preziosi, L. Modelling solid tumour growth using the theory of mixtures. *Math. Med. Biol.* **2003**, *20*, 341–366.
49. Ambrosi, D.; Preziosi, L. On the closure of mass balance models for tumor growth. *Math. Model. Methods Appl. Sci.* **2002**, *12*, 737–754.
50. Preziosi, L.; Tosin, A. Multiphase and multiscale trends in cancer modelling. *Math. Model. Nat. Phenom.* **2009**, *4*, 1–11.
51. Ambrosi, D.; Preziosi, L.; Vitale, G. The insight of mixtures theory for growth and remodeling. *Z. Angew. Math. Phys.* **2010**, *61*, 177–191.
52. Cvetković, B.P.; Kuzmanović, D.S.; Cvetković, P.A. An application of continuum theory on the case of one-dimensional sedimentation. *FME Trans.* **2011**, *39*, 61–65.
53. Nayfeh, A.H. A continuum mixture theory of heat conduction in laminated composites. *J. Appl. Mech.* **1975**, *42*, 399–404.
54. Rosi, G.; Placidi, L.; Dell'Isola, F. Fast and slow pressure waves electrically induced by nonlinear coupling in Biot-type porous medium saturated by a nematic liquid crystal. *Z. Angew. Math. Phys.* **2017**, *68*, 51–64.
55. Baer, M.R.; Nunziato, J.W. A two-phase mixture theory for the deflagration-to-detonation transition (DDT) in reactive granular materials. *Int. J. Multiph. Flow* **1986**, *12*, 861–889.
56. Kirwan, A.D. A review of mixture theory with applications in physical oceanography and meteorology. *J. Geophys. Res. Oceans* **1985**, *90*, 3265–3283.
57. Decker, R. A continuum mixture theory with an application to turbulent snow, air flows and sedimentation. *J. Wind Eng. Ind. Aerodyn.* **1990**, *36*, 877–887.
58. Del Bufalo, G.; Placidi, L.; Porfiri, M. A mixture theory framework for modeling the mechanical actuation of ionic polymer metal composites. *Smart Mater. Struct.* **2008**, *17*, 045010.
59. De Boer, R. *Trends in Continuum Mechanics of Porous Media*; Springer: New York, NY, USA, 2006.
60. Chen, P.J. A coupled solid/fluids mixture theory that suffices for diffusion problems. *J. Elast.* **1996**, *45*, 117–134.
61. Eringen, A.C. A mixture theory of electromagnetism and superconductivity. *Int. J. Eng. Sci.* **1998**, *36*, 525–543.
62. Peng, X.; Han, Y.; Huang, S. A mixture theory based constitutive model for SMA. *Mech. Res. Commun.* **2000**, *27*, 21–28.
63. Wang, L.; Wang, X.; Mohammad, L.; Wang, Y. Application of mixture theory in the evaluation of mechanical properties of asphalt concrete. *J. Mater. Civ. Eng.* **2004**, *16*, 167–174.
64. Krishnan, J.M.; Rao, C.L. Permeability and bleeding of asphalt concrete using mixture theory. *Int. J. Eng. Sci.* **2001**, *39*, 611–627.
65. Krishnan, J.M.; Rao, C.L. Mechanics of air voids reduction of asphalt concrete using mixture theory. *Int. J. Eng. Sci.* **2000**, *38*, 1331–1354.

66. Rajagopal, K.R.; Yalamanchili, R.C.; Wineman, A.S. Modeling electro-rheological materials through mixture theory. *Int. J. Eng. Sci.* **1994**, *32*, 481–500.
67. Voyiadjis, G.Z.; Song, C.R. *The Coupled Theory of Mixtures in Geomechanics with Applications*; Springer: New York, NY, USA, 2006.